MILLI-INTERACTING DARK MATTER AND THE DIRECT-SEARCH EXPERIMENTS

QUENTIN WALLEMACQ
IFPA, AGO Department, University of Liège, Sart Tilman, 4000 Liège, Belgium

Hydrogen-like dark atoms interact with standard matter because of two mixings, a kinetic mixing between standard photons and dark massless photons and a mass mixing of σ mesons and dark scalars. After having thermalized in terrestrial matter, they reach underground detectors with thermal energies and form bound states with atoms in the active media, which causes the emission of photons that produce the observed signals. The model explains well the positive results from DAMA/LIBRA and CoGeNT without any contradiction with the null results from XENON100, LUX, CDMS-II/Ge and superCDMS.

Due to the clear contradictions between direct-search experiments when they are interpreted in terms of WIMPs [1,2], alternative scenarios have been proposed to reinterpret the data. Their common feature is a complex composition of the dark sector and more sophisticated interactions with standard matter, leading to a richer phenomenology, in particular in underground detectors.

The scenario presented here is part of this rising class of models. Hydrogen-like dark atoms, bound through a dark $U(1)$ gauge coupling carried by dark massless photons, interact with terrestrial matter because of two different mixings: a kinetic mixing between the standard and the dark photon and a mass mixing between the σ meson and a neutral dark scalar. In underground detectors, after dark atoms have thermalized in terrestrial matter through elastic collisions, dark nuclei get radiatively captured by atomic nuclei of the active medium, and the emitted photons produce the observed signals.

In the following, we present the regions in the parameter space of the model that reproduce the results of DAMA/LIBRA and CoGeNT at the 2σ level, in full consistency with the null results from XENON100, LUX, CDMS-II/Ge and superCDMS. Further details about the model can be found in Refs. [3] and [4].

The dark sector is composed of two kinds of fermions, F and G, with opposite dark electric charges $+e'$ and $-e'$ respectively, that bind to from hydrogen-like dark atoms. In that system, F plays the role of a dark nucleus and G of a dark electron, i.e. $m_F \gg m_G$, where m_F and m_G are the masses of F and G. The size of these dark atoms is determined by their Bohr radius $a'_0 = 1/(m_G \alpha')$, where $\alpha' = \frac{e'^2}{4\pi}$. The massless dark photons associated with the dark $U(1)$

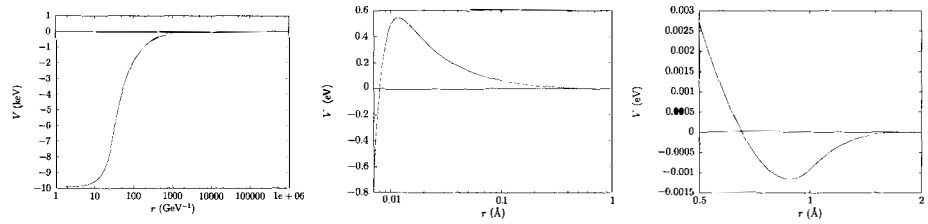

Figure 1 – Atom-dark atom potential for iodine and typical values of the parameters: $\eta = 10^{-7}$, $\epsilon = 10^{-5}$ and $m_S = 1$ MeV. Left: the whole potential. Center: a zoom on the Coulomb barrier. Right: a zoom on the atomic well.

gauge symmetry are kinetically mixed with the standard photons via the dimensionless mixing parameter ϵ. Thus, F and G have Coulomb interactions with the charged standard particles, in particular the proton and the electron, respectively with electric millicharges $+\epsilon e$ and $-\epsilon e$, where e is the charge of the proton. In addition, the dark nuclei F exchange dark neutral scalars S of mass m_S, to which they are coupled via a Yukawa coupling of strength g'. A mass mixing, characterized by a dimensionless mixing parameter η, of S with the σ meson of the standard model induces a scalar interaction between the dark nuclei and nucleons. For this attractive Yukawa-like interaction, F has a charge ηg, where g is the Yukawa coupling of the nucleon to σ.

The relevant model parameters for the direct searches are therefore m_F, m_S, η, ϵ and a'_0. However, a'_0 is fixed to 1 Å, i.e. the typical size of standard atoms, in order to have sufficiently large elastic atom-dark-atom cross sections and hence facilitate the thermalization process between the surface of the Earth and detectors located 1 km underground.

The kinetic and mass mixings produce interactions between standard and dark particles. At the atomic level, and in the non-relativistic limit, this results in a potential of interaction V between standard and dark atoms. To determine it, an atom is modelled by a finite sphere of radius 1 Å with a uniform charge distribution representing the electronic distribution. For a standard atom of atomic number Z, the total charge is $-Ze$ while it is $-\epsilon e$ for a dark one. At the center of the electronic spheres stands the nucleus, which has a finite radius, a total charge $+Ze$ and a uniform charge distribution in the case of a standard atom, whereas it is point-like and of charge $+\epsilon e$ in the dark case.

The potential is represented in Figure 1 as a function of the distance r between the two nuclei, for iodine and typical values of the parameters: $\eta = 10^{-7}$, $\epsilon = 10^{-5}$, $m_S = 1$ MeV. In the left figure, corresponding to the whole potential, we mainly see the attractive well at short distance due to the σS-exchange between nuclei, of range m_S^{-1}. A zoom at larger distance shows the Coulomb barrier at the center, due to the electrostatic repulsion betwen the two positively charged nuclei. The very shallow well on the right is the result of an attraction between the electronic cloud of an atom and the nucleus of the other, but it has no effect in the model.

Hitting the Earth, dark atoms penetrate under the surface and undergo elastic collisions with terrestrial atoms, the elastic cross section being obtained from the interaction potential V through $\left(\frac{d\sigma}{d\Omega}\right)_{el} = \frac{\mu^2}{4\pi^2}\left|\int e^{-i\vec{q}\cdot\vec{r}}V(\vec{r})\right|^2$, where μ is the reduced mass of the nucleus-F system and $\vec{q}$ is the transferred momentum. This makes them lose energy at a rate $\frac{dE}{dx}$ until they acquire thermal energies. We require that this thermalization process occurs before 1 km under the surface, which is the typical depth of underground detectors, so that the penetration length x must satisfy $x = \int_{E_{th}}^{E_0} \frac{dE}{|dE/dx|} \leq 1$ km, where the integral is performed from the incident energy E_0 to the thermal energy in the terrestrial crust $E_{th} = \frac{3}{2}T_{crust}$ with $T_{crust} \simeq 300$ K.

Afterwards, the dark atoms drift down towards the center of the Earth by gravity and arrive in detectors. The equilibrium between the incident flux at the surface of the Earth and the downfalling thermalized flux in the crust determines the number density of dark atoms in

detectors, which is annualy modulated just as the incident flux.

In a detector, dark atoms collide with atoms of the active medium and have some probability to tunnel through the Coulomb barrier of Figure 1 and hence to be captured radiatively on a bound state in the well at short distance. The transition from the continuum with energy E to this bound state of energy E_p is of electric-dipole type and since the incident plane wave, to order v/c, is mainly an s-wave, the final state of the transition has to be a p-state. This capture is accompanied by the emission of a photon of energy $|E - E_p| \simeq |E_p|$. Then, a second electric dipole transition causes the de-excitation of the nucleus-F system to a lower s-state in the well, of energy E_s, together with the emission of a photon of energy $|E_p - E_s|$. Two photons are therefore released in the detector and to avoid the observation of double-hit events, we require that the energy of the first one is below the threshold of the experiment. In principle, several transitions in the well are possible, corresponding to as many lines and hence to an emitted spectrum, but for simplicity only the transition from the lowest p-state to the ground state, which is dominant, is considered. This monochromatic line has then to lie in the detection interval, i.e. $(2-6)$ keV and $(0.5-3)$ keV respectively for DAMA and CoGeNT.

We solve the radial Schrödinger equation with the potential V for a positive energy E, which gives the radial part $R(r)$ of the initial diffusion eigenstate. Similarly, by solving the nucleus-F bound state problem, we get the radial part $R_p(r)$ of the final bound eigenfunction and the eigenstate E_p. The capture cross section σ_{capt} is then obtained by computing the matrix element $D = \int_0^\infty r R_p(r) R(r) r^2 dr$ of the dipole operator between these two states:

$$\sigma_{capt} = \frac{32\pi^2 Z^2 \alpha}{3\sqrt{2}} \left(\frac{m_F}{m_F + m} \right)^2 \frac{1}{\sqrt{\mu}} \frac{(E - E_p)^3}{E^{3/2}} D^2, \tag{1}$$

where α is the fine structure constant and m is the mass of a nucleus of the detector.

The bound-state-formation rate per unit volume is given by $R = n_F n \langle \sigma_{capt} v \rangle$, where n_F and n are the number densities of dark and standard atoms. It is obtained by averaging $\sigma_{capt} v$, where v is the relative velocity, over the velocity distributions. These are taken to be of Maxwell-Boltzmann type both for the atoms and the dark atoms, depending on the operating temperature T of the detector. Obviously, R inherits the annual modulation of n_F. The temperature T in the detector is a key parameter of the model: it allows to explain why, in two experiments made of very similar nuclei but operating at different temperatures, such as DAMA (iodine: $(Z, A) = (53, 127)$, $T \simeq 300$ K) and XENON100/LUX (xenon: $(Z, A) = (54, 132)$, $T \simeq 173$ K), only the former observes a signal. Due to the lower incident energies in the colder detector, tunneling through the Coulomb barrier will be much less efficient and hence the capture rate will be suppressed with respect to the detector operating at room temperature. A direct consequence is that this model naturally predicts no event in cryogenic detectors (CDMS-II/Ge, CDMS-II/Si, superCDMS), where temperatures $T \simeq 1$ mK are much too low to allow any tunneling.

It should be noted that the emitted photons will produce electronic recoils instead of nuclear recoils as in the usual WIMP scenario. In a detector that does not make a difference between both types of recoils, as DAMA and CoGeNT, the reinterpretation of the results is straightforward. But in XENON100, LUX or CDMS, which can clearly discriminate between electronic and nuclear recoils, there is a major difference, since the bound-state-formatrion events will be interpreted as backgrounds. If such an experiment has negative results (XENON100, LUX, CDMS-II/Ge, superCDMS), even if the rate cannot be suppressed completely, our model still predicts no detection, as the remaining events will be considered as background and rejected. We just have to ensure that the predicted electronic background is still consistent with the observed one. However, some difficulties might appear if the three events of CDMS-II/Si are confirmed, since no nuclear recoil can be produced in the model as is.

We explored the 4-dimensional parameter space of the model in order to reproduce the integrated modulation amplitudes and energy intervals of DAMA/LIBRA and CoGeNT at the 2σ level. The regions projected in two dimensions are given in Figure 2 in light red and light

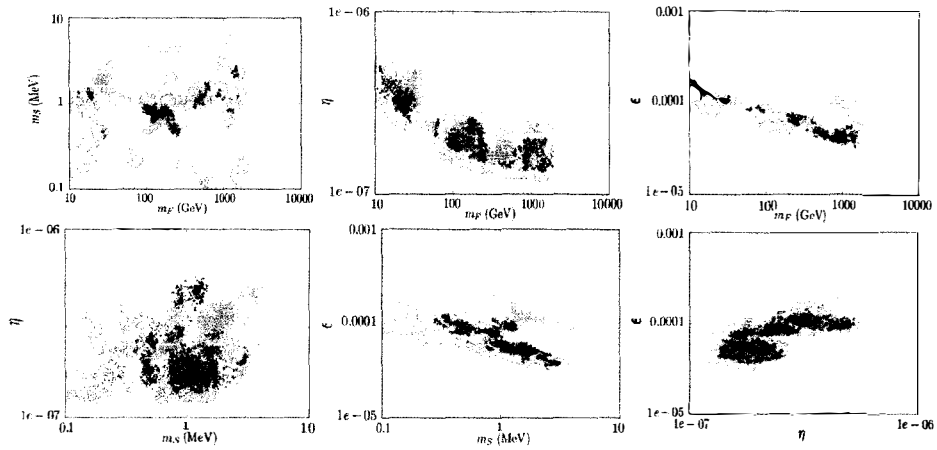

Figure 2 – Two-dimensional regions of the parameter space reproducing DAMA/LIBRA (light red) and CoGeNT (light green) at the 2σ level. Overlapping regions appear in olive green. Top left: (m_F, m_S) plane. Top center: (m_F, η) plane. Top right: (m_F, ϵ) plane. Bottom left: (m_S, η) plane. Bottom center: (m_S, ϵ) plane. Bottom right: (η, ϵ) plane.

green for DAMA/LIBRA and CoGeNT respectively, while the overlapping regions are in olive green. They show wide allowed intervals for all the parameters, with m_F going from 10 GeV to more than 1 TeV, m_S around 1 MeV, η between 10^{-7} and 10^{-6} and ϵ between 10^{-5} and 10^{-4}. We used the isotopes ^{127}I and ^{74}Ge respectively, as the detectors are made of NaI and Ge crystals. The choice of iodine instead of sodium for DAMA is to avoid the existence of bound states with light elements, i.e. the formation of heavy isotopes on Earth or during Big Bang Nucleosynthesis.

The positive results of DAMA/LIBRA and CoGeNT are consistent with the negative ones of XENON100 and LUX. By taking the models of Figure 2 and calculating the corresponding rates in liquid xenon at $T = 173$ K, we can select the ones that are consistent with the observed background. The strongest constraints on the expected and observed electron-recoil backgrounds come from LUX, but it does not really change the allowed intervals for the parameters. Finally, the predicted rates in CDMS-II/Ge and superCDMS, which are cryogenic, are consistent with zero and hence in agreement with the data.

We have briefly presented our milli-interacting dark matter model and shown the regions in its parameter space that reproduce the results of DAMA/LIBRA and CoGeNT at the 2σ level. The overlapping regions indicate wide allowed intervals for all the parameters that are in agreement with the negative results from XENON100, LUX, CDMS-II/Ge and superCDMS.

Acknowledgments

I thank the Belgian fund F.R.S-FNRS for supporting my participation to the Rencontres de Moriond 2014.

References

1. D.S. Akerib et al. *Phys. Rev. Lett.*, 112:091303, 2014.
2. R. Agnese et al. Search for Low-Mass WIMPs with SuperCDMS. 2014.
3. Quentin Wallemacq. Milli-interacting Dark Matter. *Phys. Rev.*, D88:063516, 2013.
4. Quentin Wallemacq. *Adv. High Energy Phys.*, 2014:525208, 2014.